

**Copper Coordinated Ligand Thioether-S and NO<sub>2</sub><sup>-</sup> Oxidation: Relevance to Cu<sub>M</sub> Site of Hydroxylases**

*Ram Chandra Maji<sup>a)</sup>, Anirban Bhandari<sup>a)</sup>, Ravindra Singh<sup>b)</sup>, Suprakash Roy<sup>a)</sup>, Sudip K. Chatterjee<sup>a)</sup>, Faye L. Bowles<sup>c)</sup>, Kamran B.*

*Ghiassi<sup>c)</sup>, Milan Maji<sup>a)</sup>, Marilyn M. Olmstead<sup>c)</sup>, Apurba K. Patra<sup>\*a)</sup>*

<sup>a)</sup>Department of Chemistry, National Institute of Technology Durgapur, Mahatma Gandhi Avenue, Durgapur 713 209, India

<sup>b)</sup>Department of Chemistry, Indian Institute of Technology Kanpur, Kanpur 208 016, India

<sup>c)</sup>Department of Chemistry, University of California, Davis, CA 95616 (USA)

Email: [apurba.patra.nitdgp@gmail.com](mailto:apurba.patra.nitdgp@gmail.com)

## Table of contents

<b>1</b>	<b>Fig. S1.</b> FTIR spectrum of $[(L1^{SO})Cu^{II}(ONO)]_n$ ( <b>4</b> ) in KBr disk ( $400\text{ cm}^{-1}$ - $4000\text{ cm}^{-1}$ )	
<b>2</b>	<b>Fig. S2.</b> FTIR spectrum of $[(L1)Cu^{II}(NO_3)]_n$ ( <b>5</b> ) in KBr disk ( $400\text{ cm}^{-1}$ - $4000\text{ cm}^{-1}$ )	
<b>3</b>	<b>Fig. S3.</b> FTIR spectrum of $[(L1^{SO})Cu^{II}(NO_3)]_n$ ( <b>6</b> ) in KBr disk ( $400\text{ cm}^{-1}$ - $4000\text{ cm}^{-1}$ )	
<b>4</b>	<b>Fig. S4.</b> $^1\text{H-NMR}$ spectrum of $L1^{SO}$ in $\text{CDCl}_3$ .	
<b>5</b>	<b>Fig. S5.</b> ESI positive mass spectra of $L1^{SO}$ taken in $\text{CHCl}_3$	
<b>6</b>	<b>Fig. S6.</b> ESI positive mass spectra of $L1^{SO2}$ taken in $\text{CHCl}_3$	
<b>7</b>	<b>Fig. S7.</b> Cyclic voltammogram of HL1 in $\text{CH}_3\text{CN}$	
<b>8</b>	<b>Fig. S8.</b> Cyclic voltammogram of $[(L1)Cu^{II}(NO_3)]_n$ ( <b>5</b> ) in $\text{CH}_3\text{CN}$	
<b>9</b>	<b>Fig. S9.</b> Cyclic voltammogram of $[(L1^{SO})Cu^{II}(NO_3)]_n$ ( <b>6</b> ) in $\text{CH}_3\text{CN}$	
<b>10</b>	<b>Fig. S10.</b> Cyclic voltammogram of $\{[(L1^{SO})Cu^{II}(\text{CH}_3\text{CN})](\text{ClO}_4)\}_n$ , ( <b>2</b> ) in $\text{CH}_3\text{CN}$	
<b>11</b>	<b>Fig. S 11:</b> Electronic absorption spectral changes $[(L1)Cu^{II}(ONO)]_n$ ( <b>3</b> ) +1 $\text{H}_2\text{O}_2$	
<b>12</b>	<b>Fig. S12:</b> 3-D Polymeric structure of $[(L1^{SO})Cu^{II}(NO_3)]_n$ ( <b>6</b> )	

<b>13</b>	<b>Fig. S13:</b> Mechanism of reference 2(b)	
<b>14</b>	<b>Fig. S14:</b> Cyclic voltammogram of [(L1)Cu <sup>II</sup> (NO <sub>3</sub> )] ( <b>5</b> ) and <b>5</b> + 40 equiv NaNO <sub>3</sub>	
<b>15</b>	<b>Fig. S15:</b> Cyclic voltammogram of [(L1)Cu <sup>II</sup> (NO <sub>3</sub> )] ( <b>6</b> ) and <b>6</b> + 40 equiv NaNO <sub>3</sub>	
<b>16</b>	<b>Fig. S16:</b> Cyclic voltammogram of [(L1)Cu <sup>II</sup> (NO <sub>3</sub> )] ( <b>7</b> ) and <b>7</b> + 40 equiv NaNO <sub>3</sub>	
<b>17</b>	<b>Fig. S17.</b> X-band EPR spectra of [(L1)Cu <sup>II</sup> (NO <sub>2</sub> )] ( <b>3</b> ) in MeCN-toluene at 298 K and 77 K	
<b>18</b>	<b>Fig. S18.</b> X-band EPR spectra of [(L1)Cu <sup>II</sup> (NO <sub>3</sub> )] ( <b>5</b> ) in MeCN-toluene at 298 K and 77 K	
<b>19</b>	Crystallographic details of <b>4-6</b> and <b>2</b> as CIF files	

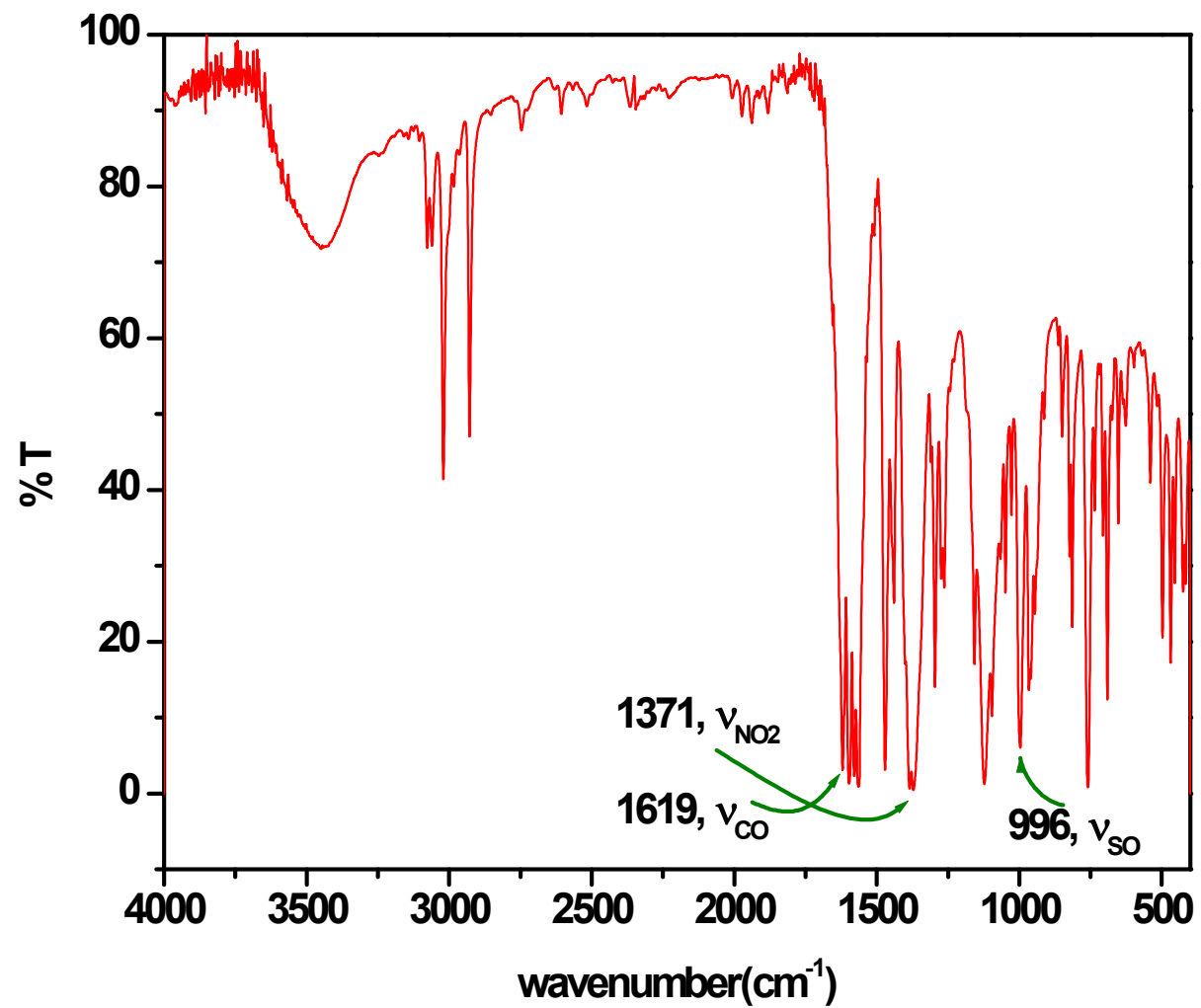


**Fig. S1.** FTIR spectrum of  $[(L1^{SO})Cu^{II}(ONO)]$  (4) in KBr disk ( $400\text{ cm}^{-1}$ - $4000\text{ cm}^{-1}$ )

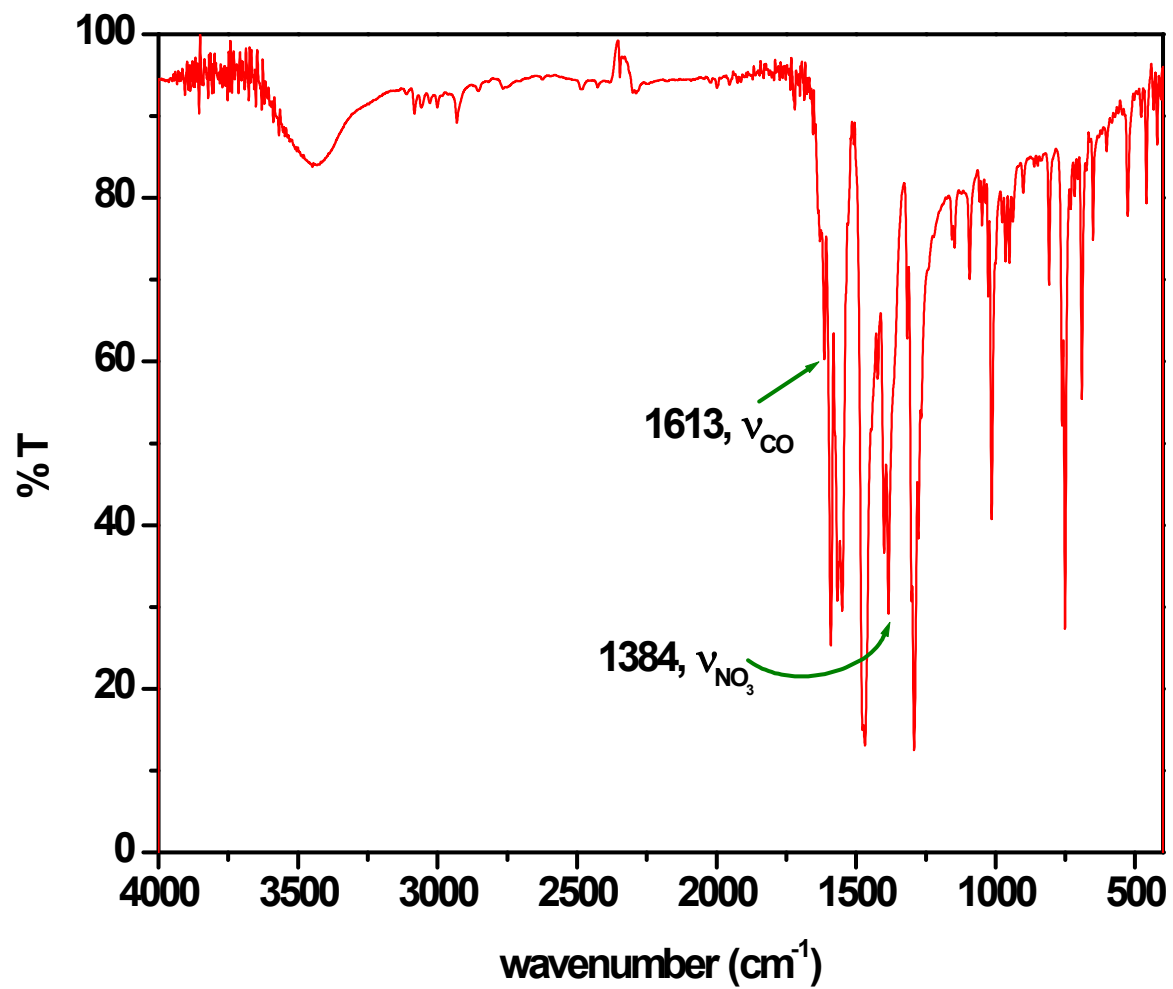


**Fig. S2.** FTIR spectrum of  $[(L1)Cu^{II}(NO_3)]$  (5) in KBr disk ( $400\text{ cm}^{-1}$ - $4000\text{ cm}^{-1}$ )

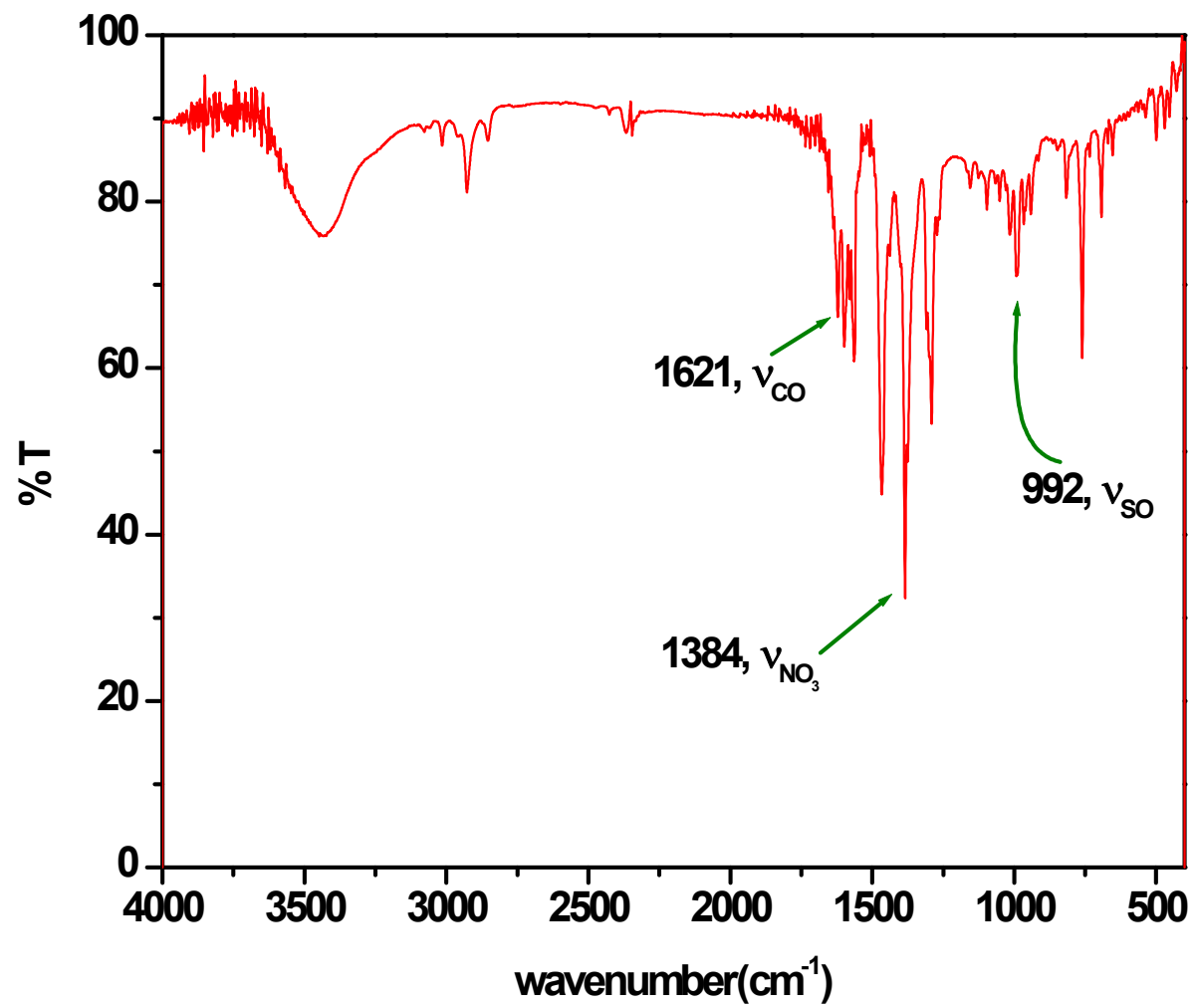


**Fig. S3.** FTIR spectrum of  $[(L1^{S^O})Cu^{II}(NO_3)]$  (6) in KBr disk ( $400\text{ cm}^{-1}$ - $4000\text{ cm}^{-1}$ )

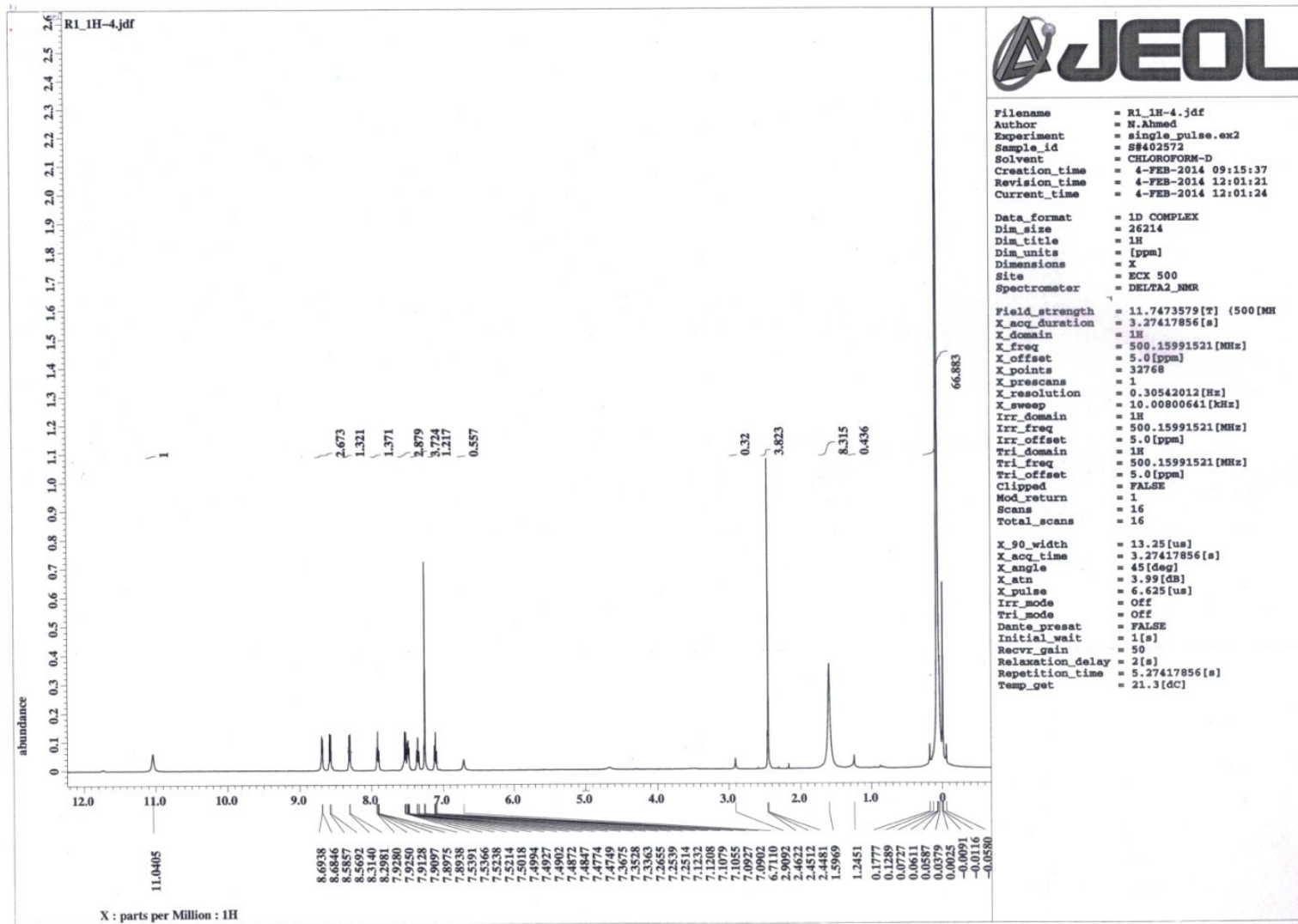
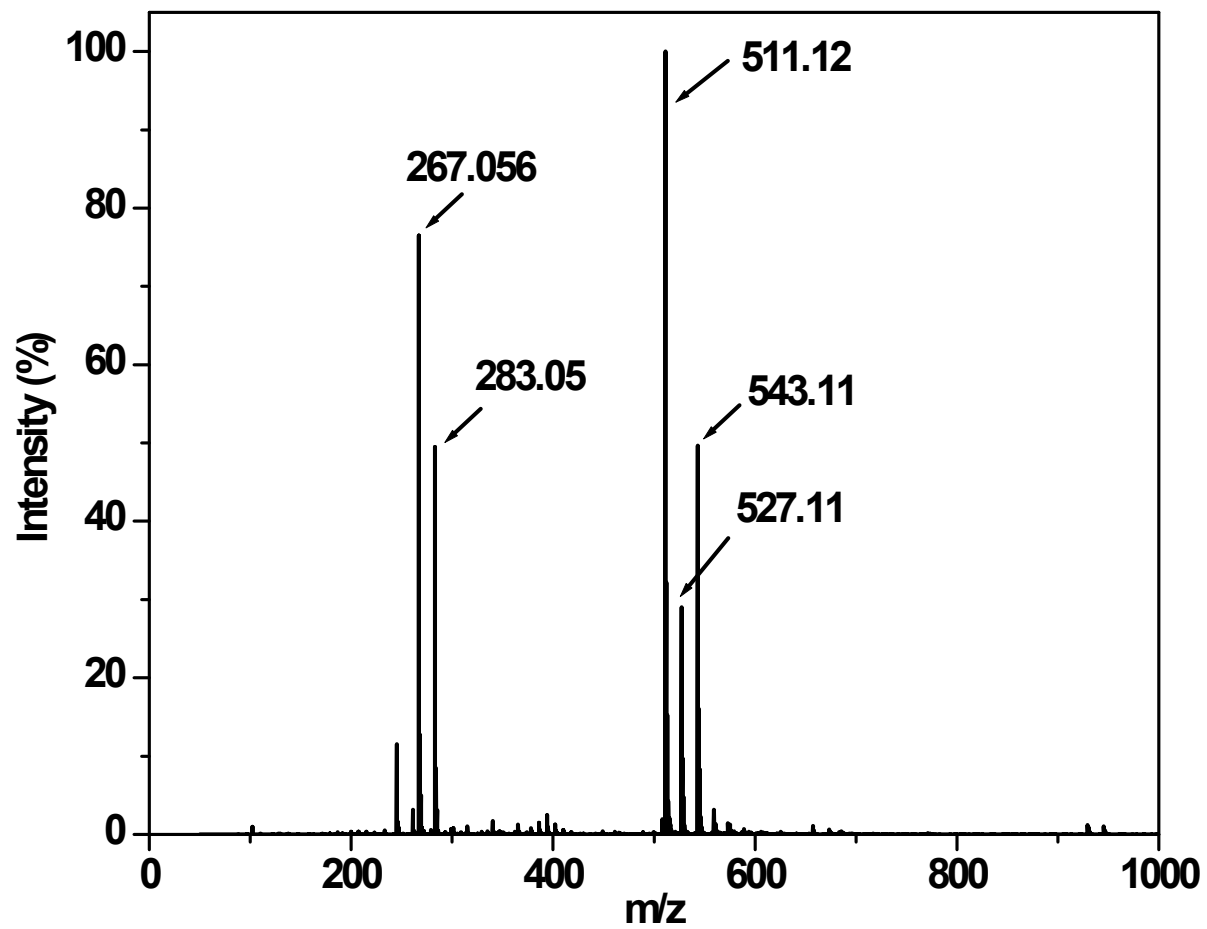


Fig. S4.  $^1\text{H}$ -NMR spectrum of  $\text{L1}^{\text{SO}}$  in  $\text{CDCl}_3$ .



**Fig. S5.** ESI positive mass spectrum of **HL1<sup>SO</sup>** taken in **CHCl<sub>3</sub>**.

**283:**  $\{L1^{SO} + Na\}^+$ , **267:**  $\{L1^{SO}-O + Na\}^+$ , **543:**  $\{(L1^{SO})_2 + Na\}^+$ , **527:**  $\{(L1^{SO})_2-O + Na\}^+$ , **511:**  $\{(L1^{SO})_2-2O + Na\}^+$



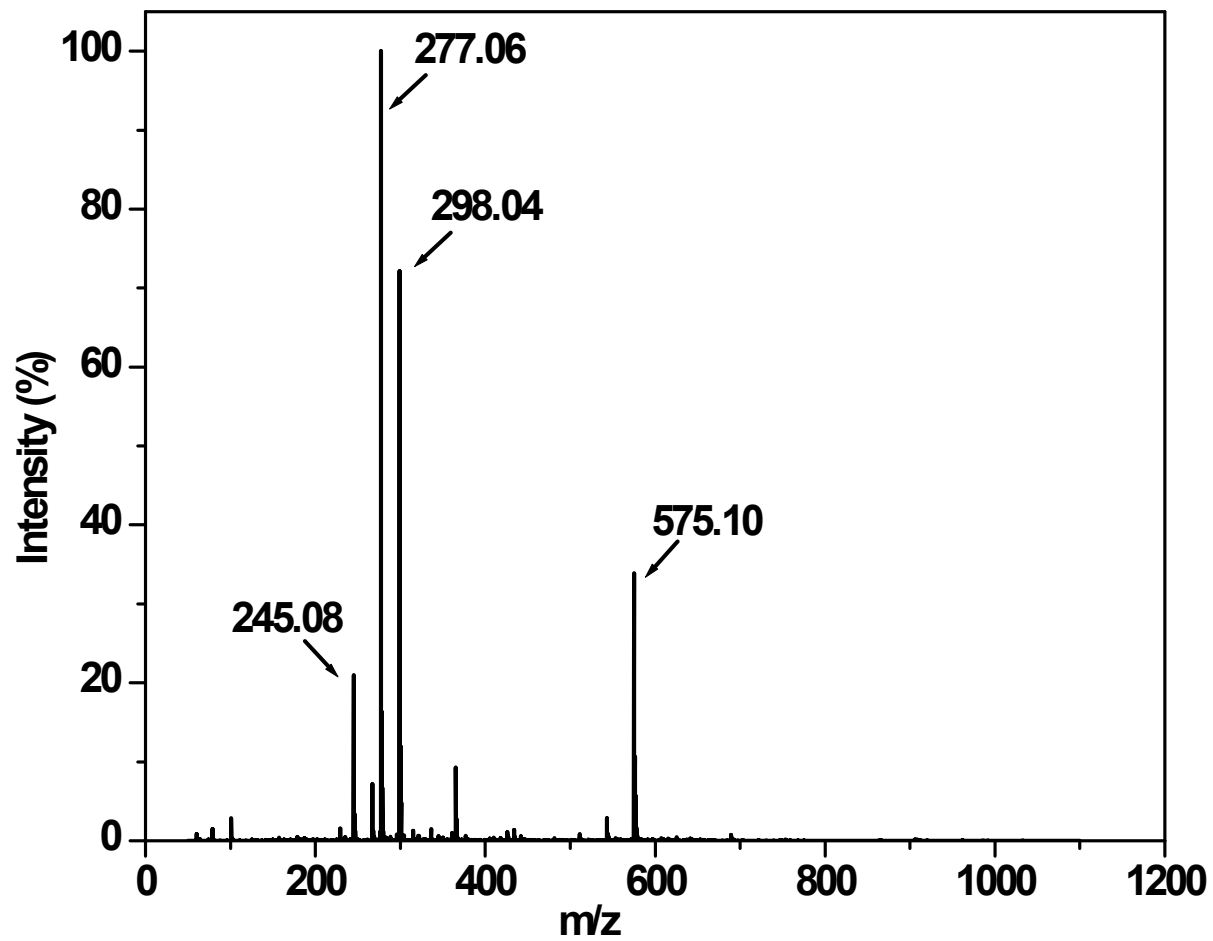


**Fig. S6.** ESI positive mass spectrum of  $\text{HL1}^{\text{SO}_2}$  taken in  $\text{CHCl}_3$ .

**277:**  $\{\text{L1}^{\text{SO}_2} + \text{H}\}^+$ , **298:**  $\{\text{L1}^{\text{SO}_2} + \text{Na}\}^+$ , **575:**  $\{(\text{L1}^{\text{SO}_2})_2 + \text{Na}\}^+$ , **244:**  $\{\text{L1}^{\text{SO}_2} - 2\text{O}\}^+$

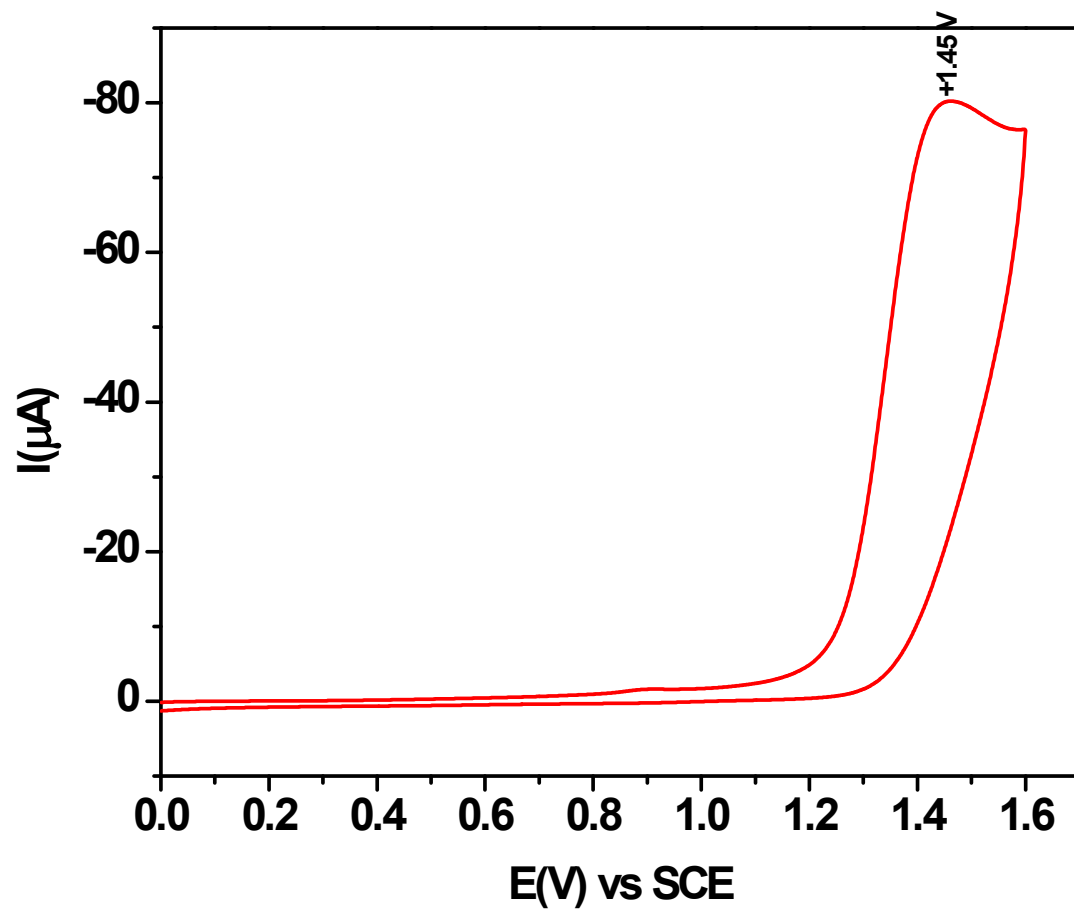


**Fig. S7.** Cyclic voltammogram of **HL1** in  $\text{CH}_3\text{CN}$  containing  $(\text{Bu}_4\text{N})\text{ClO}_4$  as supporting electrolyte at 298 K at Pt working electrode at a scan rate of 50 mV/s using SCE reference electrode.

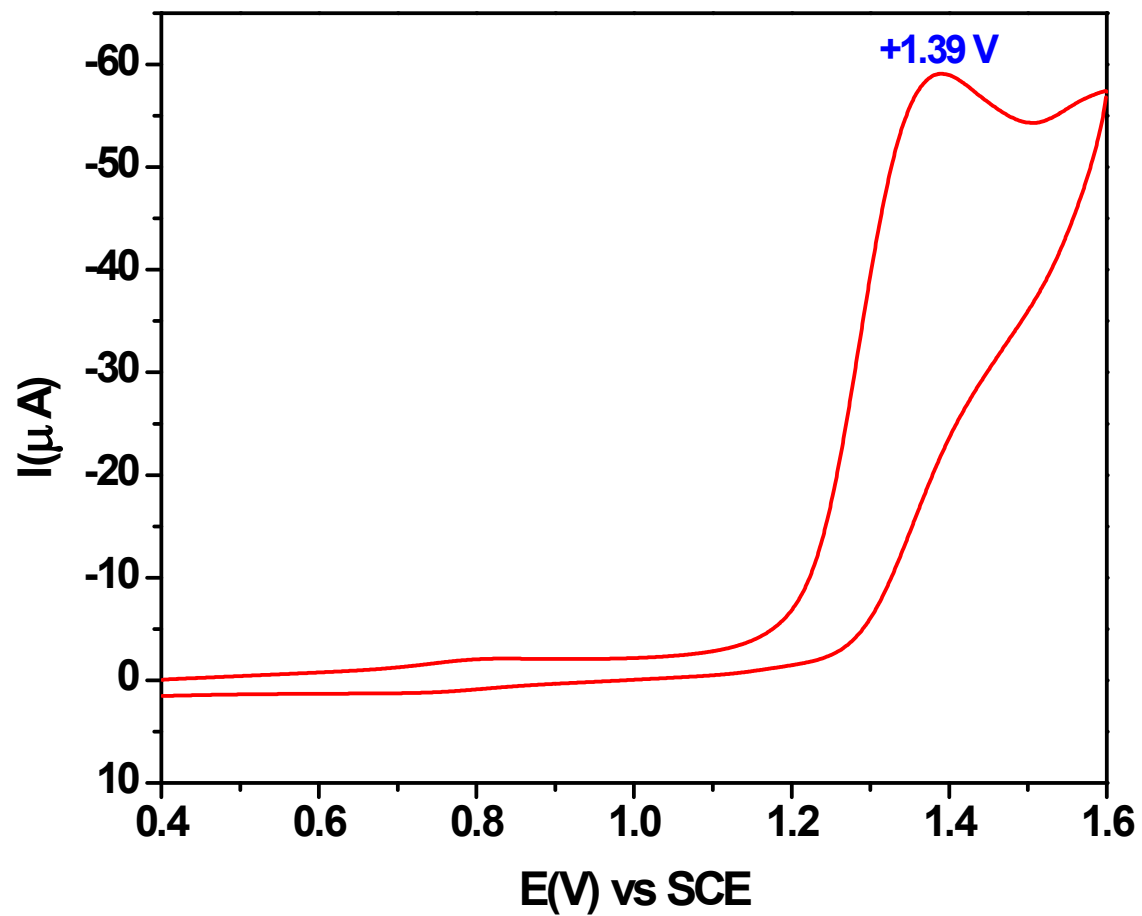


**Fig. S8.** Cyclic voltammogram of  $[(L1)Cu^{II}(NO_3)]$  (**5**) in  $CH_3CN$  containing  $(Bu_4N)ClO_4$  as supporting electrolyte at 298 K at Pt working electrode at a scan rate of 50 mv/s using SCE reference electrode.

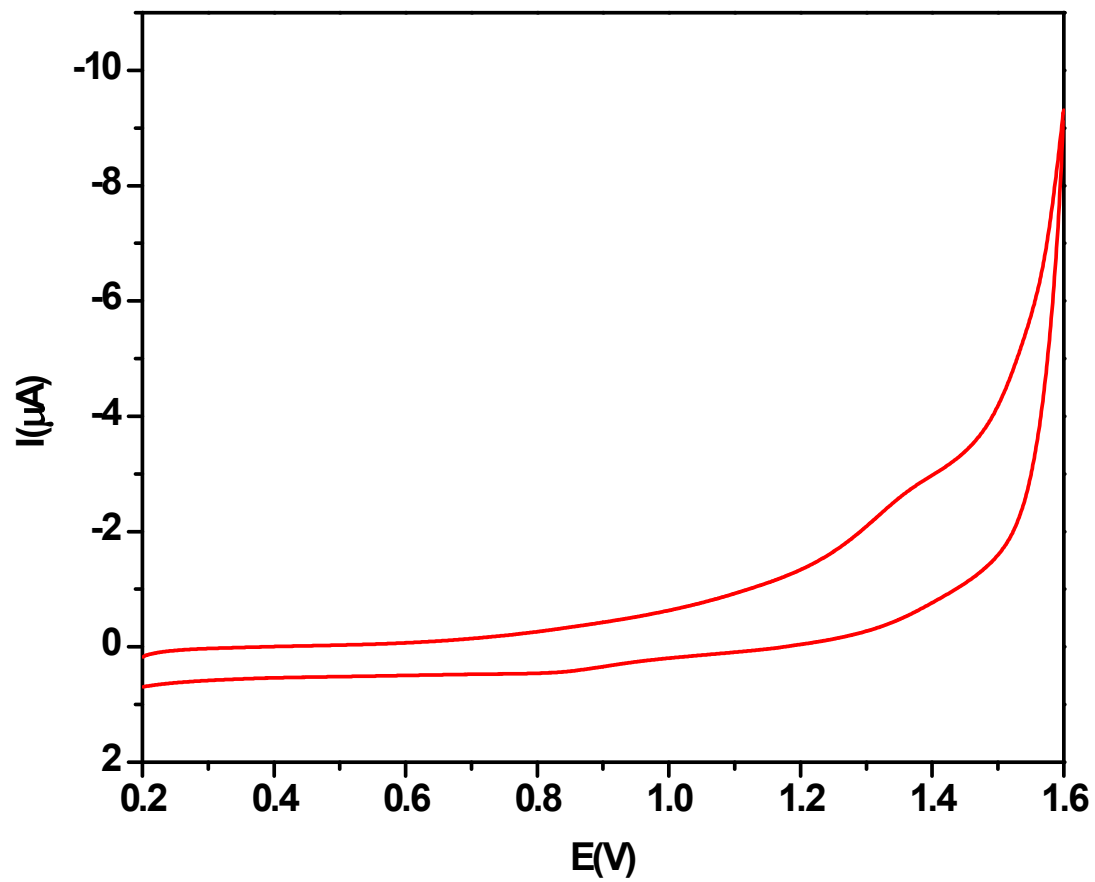


**Fig. S9.** Cyclic voltammogram of  $[(\text{L1}^{\text{SO}})\text{Cu}^{\text{II}}(\text{NO}_3)]$  (**6**) in  $\text{CH}_3\text{CN}$  containing  $(\text{Bu}_4\text{N})\text{ClO}_4$  as supporting electrolyte at 298 K at Pt working electrode at a scan rate of 50 mV/s using SCE reference electrode.

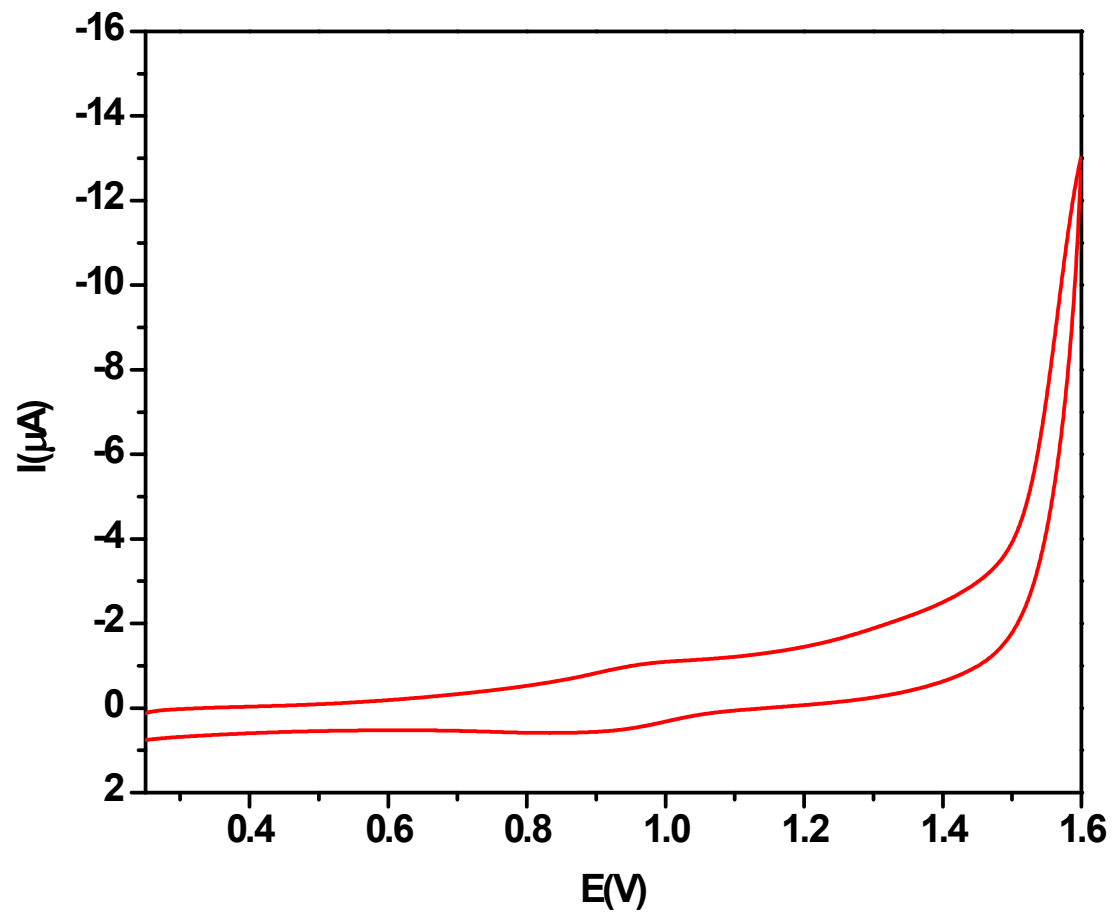


**Fig. S10.** Cyclic voltammogram of  $[(L1^{S0})Cu^{II}(CH_3CN)](ClO_4)$ , (2) in  $CH_3CN$  containing  $(Bu_4N)ClO_4$  as supporting electrolyte at 298 K at Pt working electrode at a scan rate of 50 mv/s using SCE reference electrode.

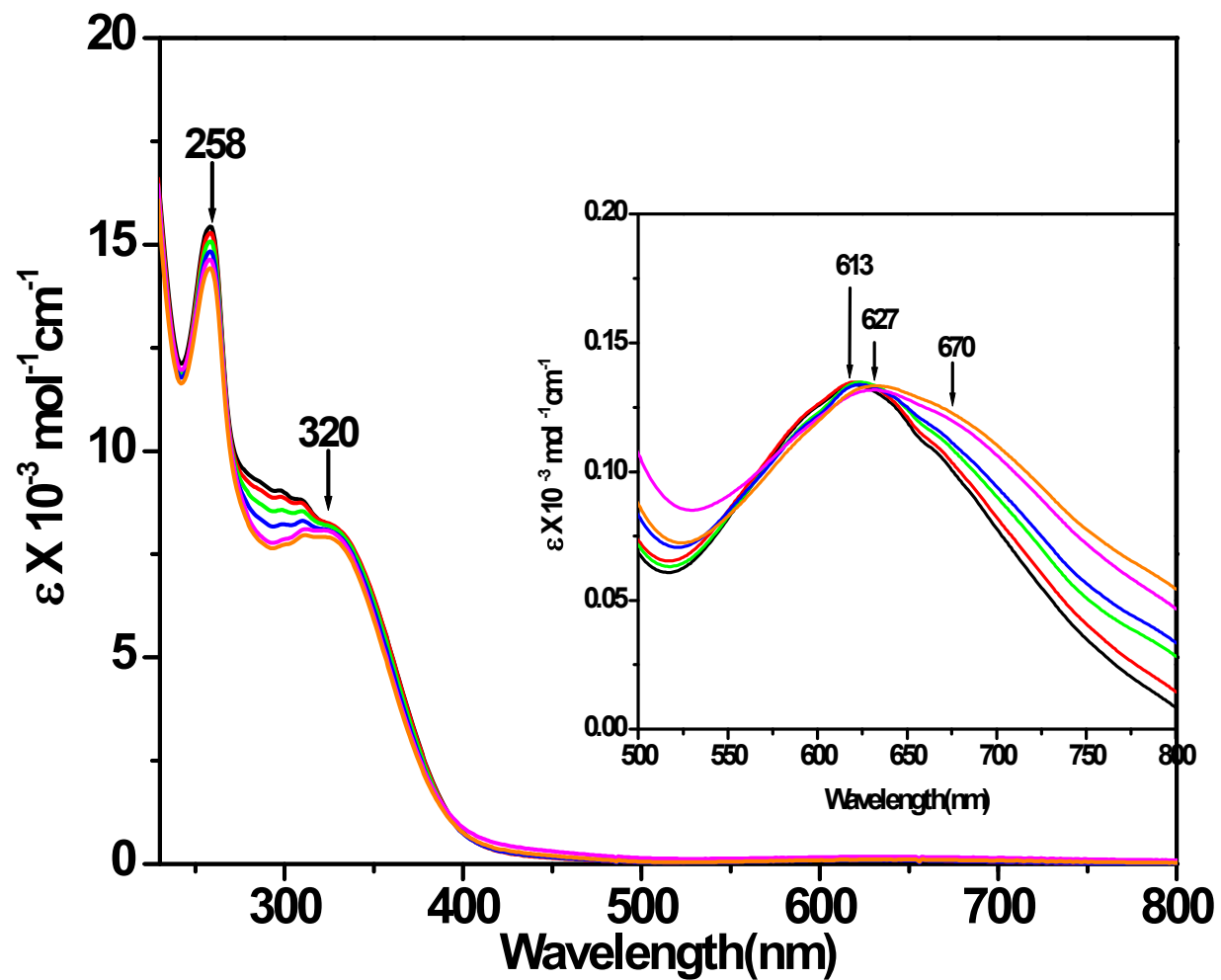


**Fig. S 11:** Electronic absorption spectral changes when titrating a  $\text{CH}_3\text{CN}$  solution of  $[(\text{L1})\text{Cu}^{\text{II}}(\text{ONO})]$  (3) with a  $\text{CH}_3\text{CN}$  solution of one equivalent  $\text{H}_2\text{O}_2$ .

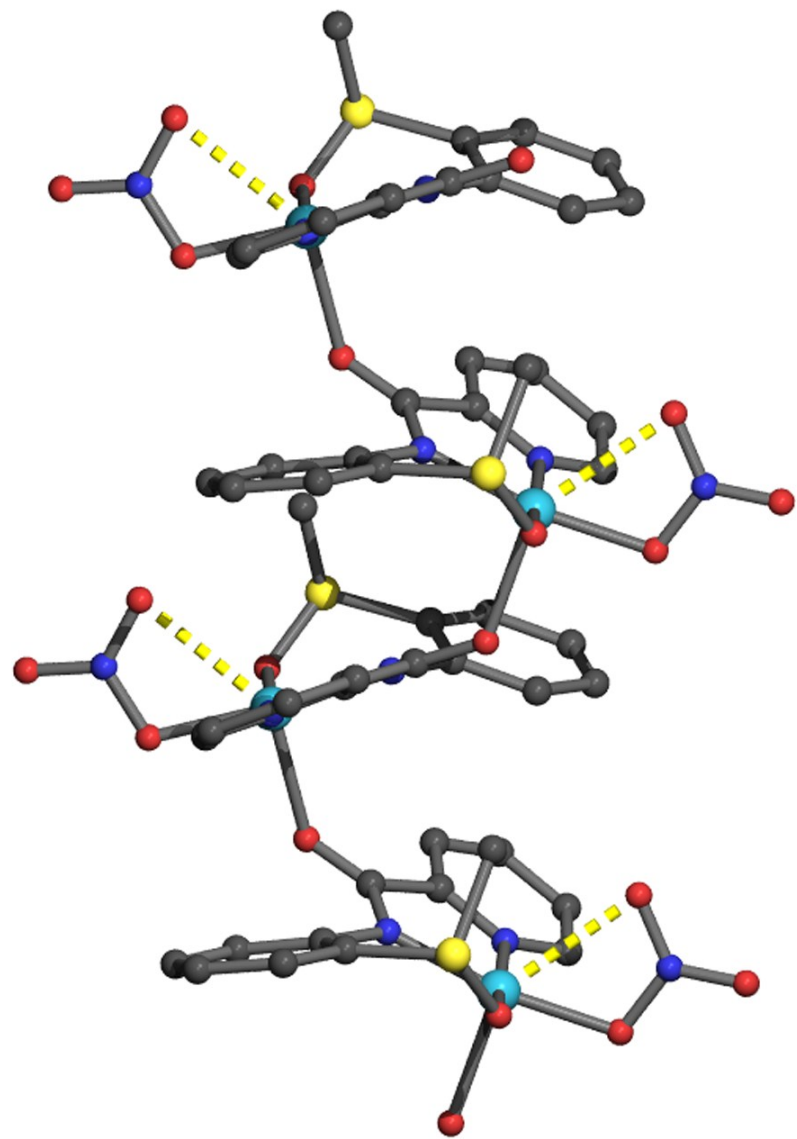


**Fig. S12:** 3-D Polymeric structure of  $[(L1^{SO})Cu^I(NO_3)]$  (6)

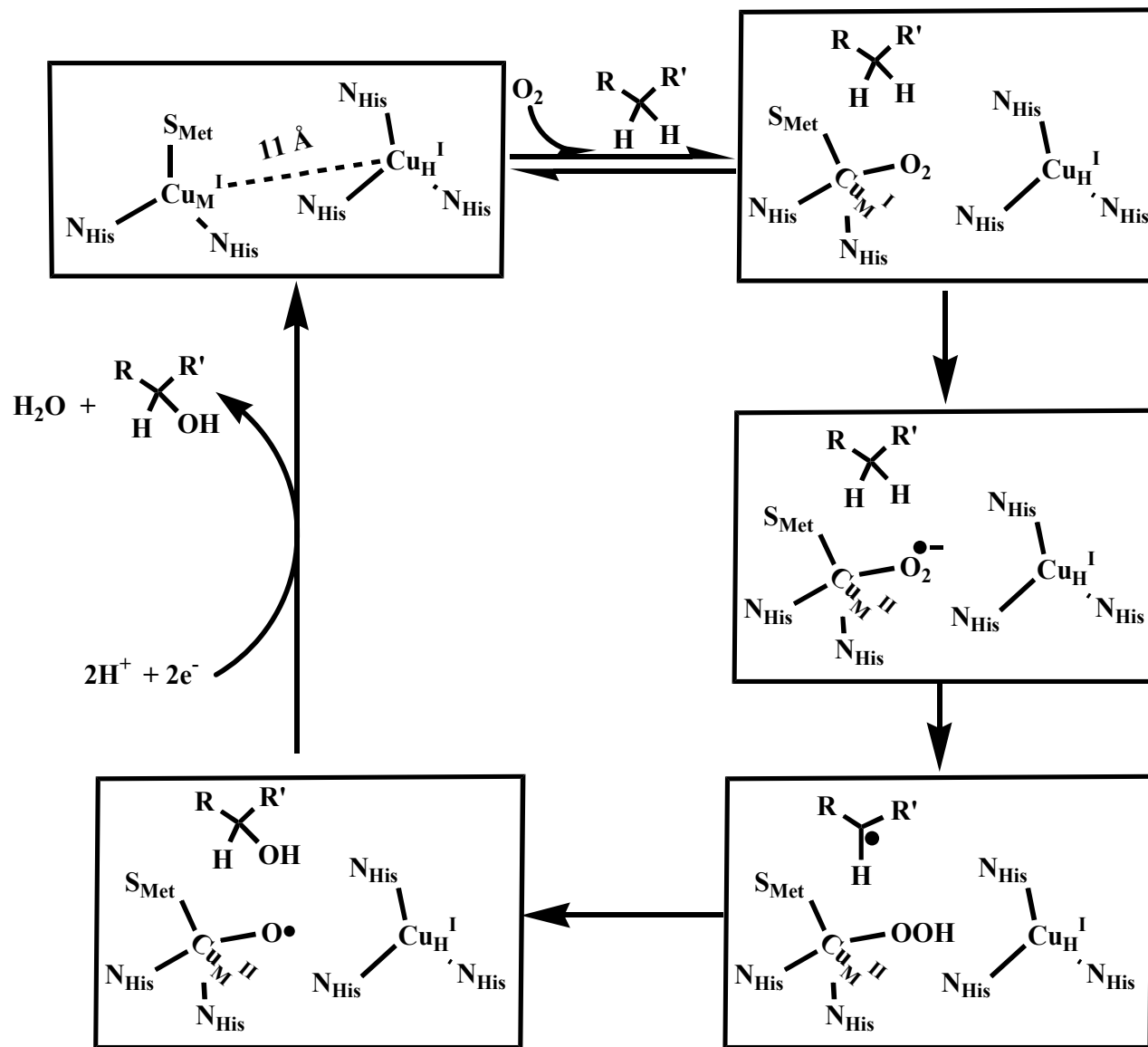
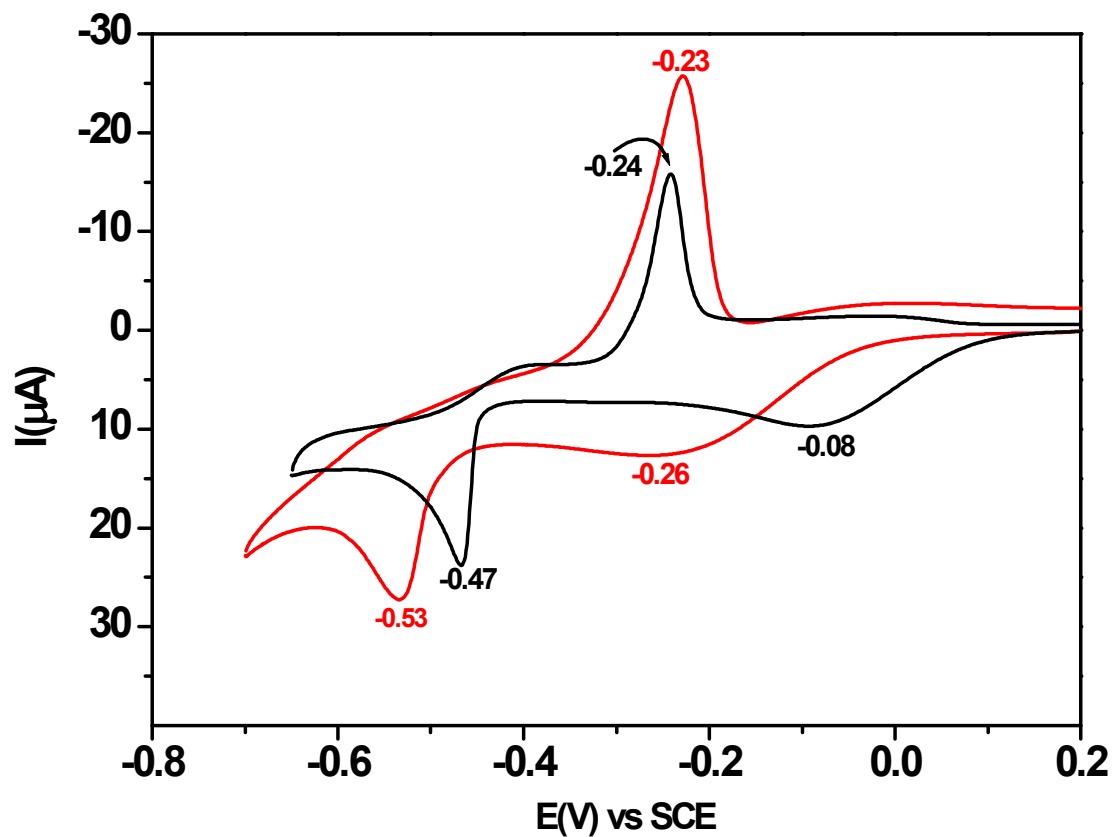
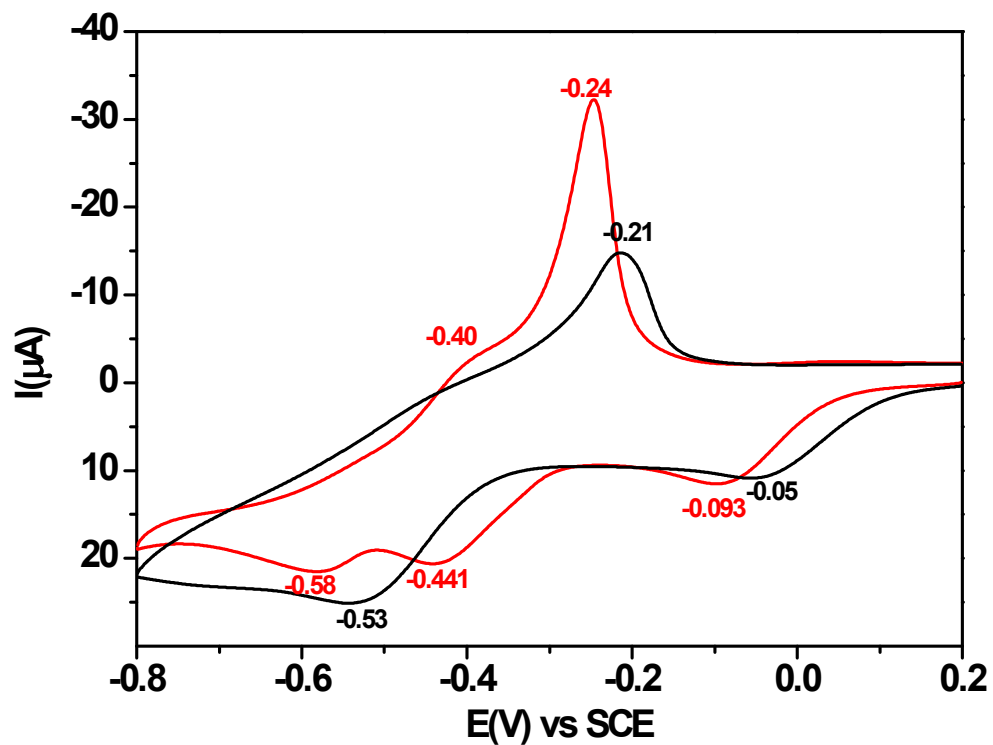


Fig. S13: Proposed mechanistic pathway for C-H hydroxylation, adopted from ref 2(b)





**Fig. S14:** Cyclic voltammogram of  $[(L1)Cu^{II}(NO_3)]$  (**5**) (black trace) and (**5** + 40 equiv.  $NaNO_3$ , red trace) in 1:100 v/v  $H_2O/CH_3CN$  mixed solvent containing  $(Bu_4N)ClO_4$  as supporting electrolyte at 298 K at Pt working electrode at a scan rate of 50 mV/s using SCE reference electrode.



**Fig. S15:** Cyclic voltammogram of  $[(\text{L}1^{\text{SO}})\text{Cu}^{\text{II}}(\text{NO}_3)]$  (**6**) (black trace) and (**6** + 40 equiv.  $\text{NaNO}_3$ , red trace) in 1:100 v/v  $\text{H}_2\text{O}/\text{CH}_3\text{CN}$  mixed solvent containing  $(\text{Bu}_4\text{N})\text{ClO}_4$  as supporting electrolyte at 298 K at Pt working electrode at a scan rate of 50 mv/s using SCE reference electrode.

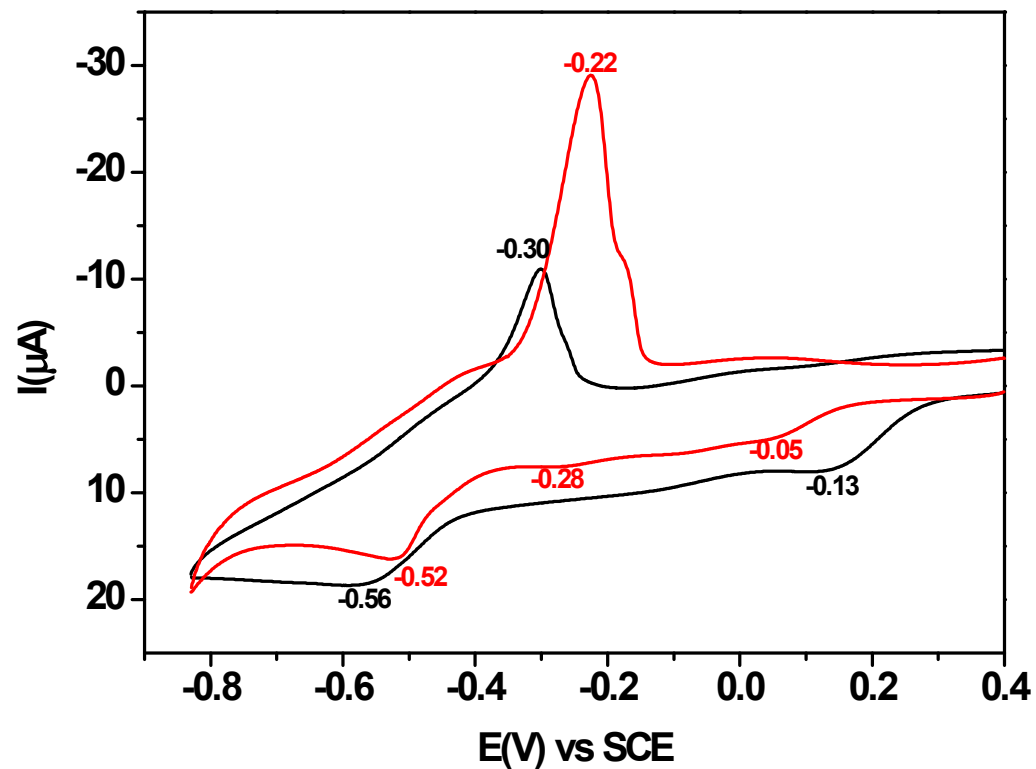


**Fig. S16:** Cyclic voltammogram of  $[(L1^{SO_2})Cu^{II}(NO_3)]$  (**7**) (black trace) and (**7** + 40 equiv.  $NaNO_3$ , red trace) in 1:100 v/v  $H_2O/CH_3CN$  mixed solvent containing  $(Bu_4N)ClO_4$  as supporting electrolyte at 298 K at Pt working electrode at a scan rate of 50 mv/s using SCE reference electrode.

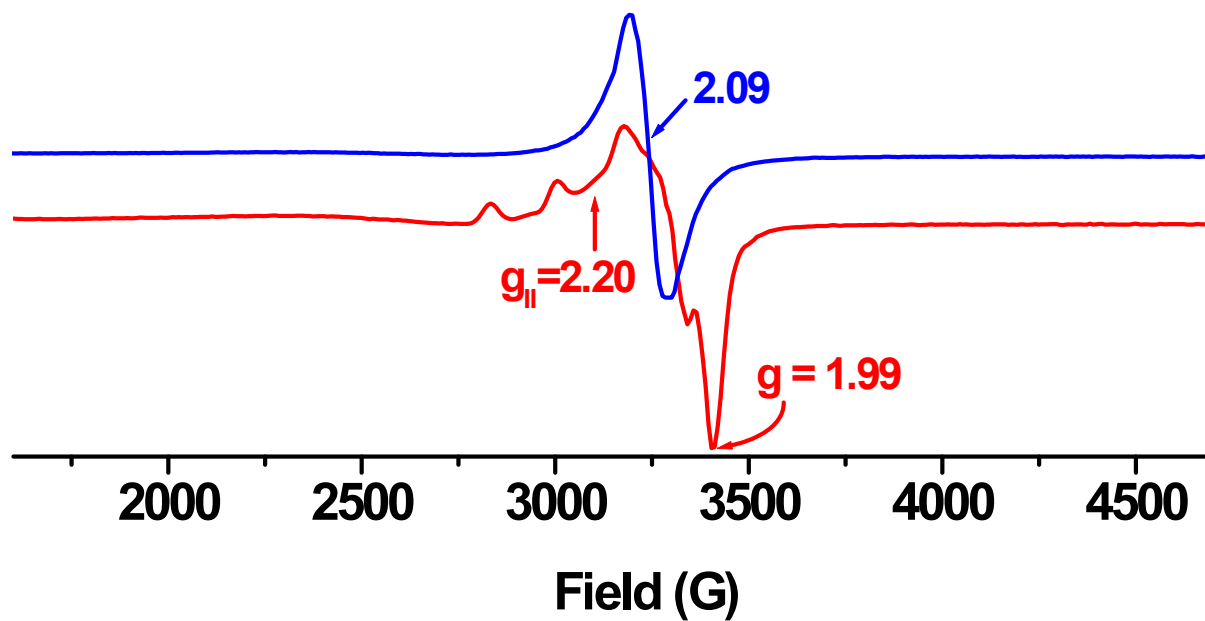


**Fig. S17.** X-band EPR spectra of  $[(L1)Cu^{II}(NO_2)]$  (**3**) in MeCN-toluene at 298 K (blue trace) and at 77 K (red trace)

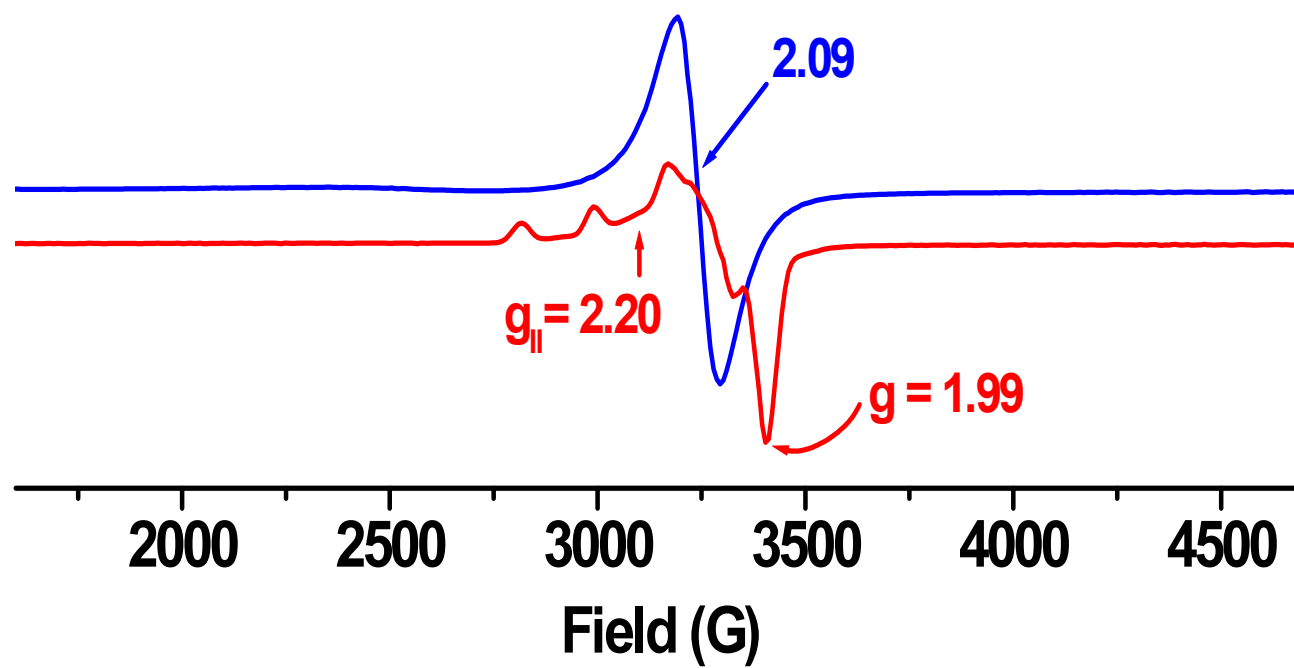


**Fig. S18.** X-band EPR spectra of  $[(L1)Cu^{II}(NO_3)]$  (**5**) in MeCN-toluene at 298 K (blue trace) and at 77 K (red trace)